www.flame-structure-2014.com

Berlin Institute of Technology (TU Berlin)

Prof. Dr. Frank Behrendt
Fakultät III: Prozesswissenschaften,
Institut für Energietechnik

Chair Energy Process Engineering and Conversion Technologies for Renewable Energies (EVUR)
Fasanenstr. 89
10623 Berlin

Contact
info@flame-structure-2014.com
frank.behrendt@tu-berlin.de

10. Juni 14

Berlin Institute of Technology • Fasanenstr. 89 • 10623 Berlin

German Aerospace Centre (DLR),
Institute of Combustion Technology
Dr. Nadezda Slavinskaya
Pfaffenwaldring 38-40
70569 Stuttgart, Germany

Confirmation of paper submission

Name:	Dr. Nadezda Slavinskaya
Email:	nadja.slavinskaya@dlr.de
Co-author:	D.A. Knyazkov
2nd co-author:	A.M. Dmitriev
3rd co-author:	A.G. Shmakov, O.P. Korobeinichev, U.Riedel
Title of Paper:	Fuel-Rich Premixed n-Heptane/Toluene Flame: A Molecular Beam Mass Spectrometry and Chemical Kinetic Study
Program:	Kinetics
Name of Institute:	German Aerospace Centre (DLR), Institute of Combustion Technology

Fuel-Rich Premixed n-Heptane/Toluene Flame: A Molecular Beam Mass Spectrometry and Chemical Kinetic Study

N.A. Slavinskaya[3*], D.A. Knyazkov[1,2], A.M. Dmitriev[1,2], A.G. Shmakov[1,2], O.P. Korobeinichev[1], U.Riedel[3]

[1] Voevodsky Institute of Chemical Kinetics and Combustion, Novosibirsk, Russia
[2] Novosibirsk State University, Novosibirsk, Russia
[3]German Aerospace Centre (DLR), Institute of Combustion Technology, Stuttgart, Germany

Practical hydrocarbon fuels are complex mixtures of several hundreds of individual species. Their models are mostly established to contain the species from 4 main families of hydrocarbons (n/i- paraffins, naphthenes, aromatics) and to predict various combustion characteristics and pollution formation. As the mixture of simplest substituted aromatic (C_7H_8, toluene) and "smallest" large n-paraffin (n-C_7H_{16}, n-heptane) used in fuel blends, this combination can be effectively used for an investigation of specifics of the poly-aromatic hydrocarbon (PAH) formation and growth in engines.

In this study, we report the newly measured mole fraction profiles including PAH precursors in an atmospheric premixed burner-stabilized fuel-rich (φ=1.75) n-heptane/toluene/O_2/Ar flame (n-heptane/toluene ratio is 7:3 by liquid volume). An extended reaction mechanism constructed on the basis of a detailed mechanism [1-3] is used to simulate the experimental data. The histories of reactions of aromatic molecule formation are examined and discussed.

Chemical kinetic mechanism formulation

The reaction model used for the n-heptane/toluene mixture oxidation is a part of the global reaction data base at the DLR Institute of Combustion Technology. This kinetic data base has a hierarchical structure and is developed through continuous adaptation, extension, validation and optimization. The reaction database includes an inherently consistent body reaction model with submodels for H_2, CO, CH_4, CH_3OH, C_2H_4, C_2H_5OH, C_2H_6, C_3H_8, n-C_4H_{10}, C_7H_8, cy-C_6H_{12}, cy-C_9H_{18}, n-C_7H_{16}, i-C_8H_{18}, n-$C_{10}H_{22}$, i-$C_{10}H_{22}$, i-$C_{11}H_{24}$, n-$C_{12}H_{26}$ and n-$C_{16}H_{34}$. The core detailed reaction model consists of C_1-C_2 mechanism with PAH formation [1-3]. Figures 1 illustrates the model facilities to reproduce the laminar flame speed s of studied fuels. Figures 2 and 3 show a comparison of mole fraction profiles and soot volume fractions measured in a laminar premixed n-heptane [9] and toluene flame [10] with the model predictions.

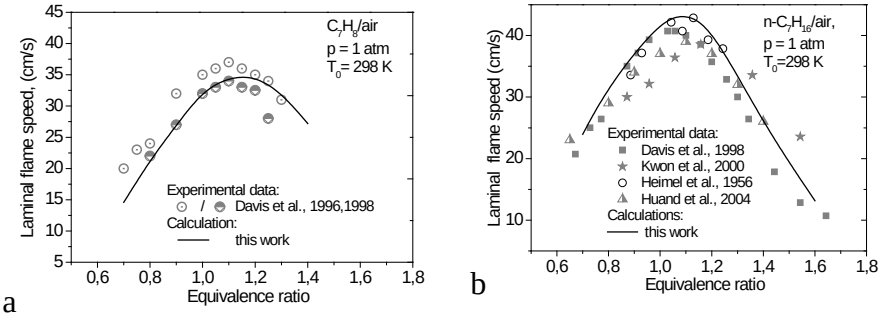

Fig.1. Comparisons of experimental data and simulation results for laminar flame speed of toluene [4] a) and n-heptane [5-8] (b).

Experimental details

A fuel-rich premixed flame of n-heptane/toluene/O_2/Ar is stabilized on a Botha-Spalding flat burner at atmospheric pressure. The burner consists of a perforated (0.5 mm orifices with 0.7 mm center-to-center spacing) brass disc 16 mm in diameter and 3 mm thick embedded in a brass housing surrounded by a jacket for the circulation of a thermostating liquid (polymethylsiloxane temperature kept at 120°C). The flows of argon and oxygen are adjusted by the calibrated mass-flow controllers (MKS Instruments Inc.). n-Heptane and toluene are premixed (liquids volume ratio was 7:3, respectively) and supplied into a vaporizer through a steel capillary using a syringe pump driven by a stepper motor. The line between the vaporizer and the burner has an inlet for the oxygen supply to the gaseous n-heptane/toluene/Ar mixture. This line is maintained at 120^0C by an electrical heater. The temperatures of the burner housing, the line, and the vaporizer are controlled by T-type thermocouples. The flame has the following mole composition: n-heptane/toluene /O_2/Ar =

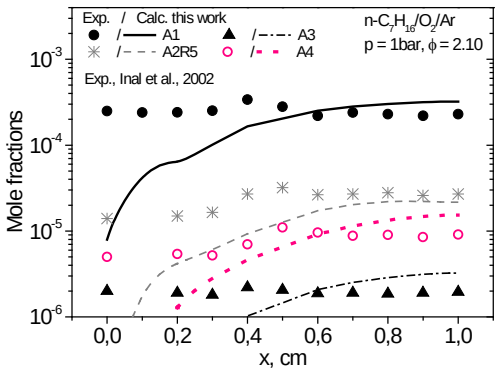

Fig.2. Comparison of mole fraction profiles of aromatic molecules measured in a laminar premixed n-heptane/O_2/Ar flame [9] with the model predictions.

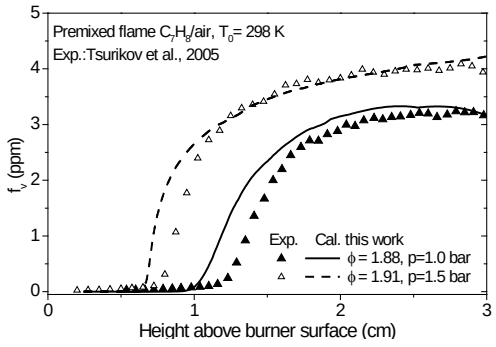

Fig.3. Soot volume fractions measured in the laminar premixed toluene/air flame [10] compared against simulations.

2.29/1.36/21.36/75 % (equivalence ratio φ=1.75). The total flow rate of the unburnt mixture is 0.92 slpm. Flame sampling molecular beam mass spectrometry (MBMS) with soft ionization by electron impact is used for measurements of species mole fractions in the flame as a function of the height above burner (HAB). Detailed description of the MBMS setup is given elsewhere [11]. It has been used previously to measure atmospheric-pressure flame structures, see, e.g., [12]. Flame sample is extracted from the burning area by a quartz cone nozzle with 40° inner angle and 0.08 mm orifice diameter. The wall thickness at the nozzle tip is 0.08 mm to minimize heat loss from the sampling area into the nozzle and to produce minimal flame perturbations. The gas sample forms a molecular beam that passes through a skimmer, molecular beam modulator and collimator before entering a region of soft ionization by electrons (spread in ionization energies of ±0.25 eV, the basis width of the electron energy distribution function). Ions are collected and analyzed by a quadrupole mass-spectrometer. Electron energies are selected for each species analyzed in order to obtain a signal-to-noise ratio high enough, without interferences from fragmentation of other species. Deriving mole fraction profiles for intermediate species from the mass peak intensity profiles has been achieved using the procedure proposed by Cool et al. [13]. A similar procedure was used and described in details in our previous work [12], and it is described only briefly below. The uncertainty of the determination of mole fraction of the flame reactants and major products (CO, CO_2, H_2O, H_2) is estimated to be ±15% of the maximum mole fraction values. For other species, mole fractions are determined to within a factor of about 2. Temperature profiles in the flames are measured by a Pt/Pt+10%Rh thermocouple with SO2 anticatalytic coating. The procedure of its manufacturing as well as its dimensions is described in [12]. The flame temperature profile is measured with the thermocouple junction located at 0.2 mm from the sampling nozzle tip. The radiation heat losses by the thermocouple are taken into account as described elsewhere [14-15]. The measured temperature profiles were used as input data for the flame structure simulations. Gas-dynamic perturbations of the flame by the sampling probe were taken into account similarly as it was done in our previous works [12, 15] by shifting all the mole fraction profiles measured upstream by the distance $Z \sim d \cdot (Q/(S \cdot V))^{0.5}$, where d is the diameter of the orifice, Q is the volumetric flow rate though the orifice, S is the area of the orifice and V is the linear velocity of the flow riding onto the probe [16]. The maximum shift corresponds to the position of the probe near the burner and does not exceed 0.3 mm.

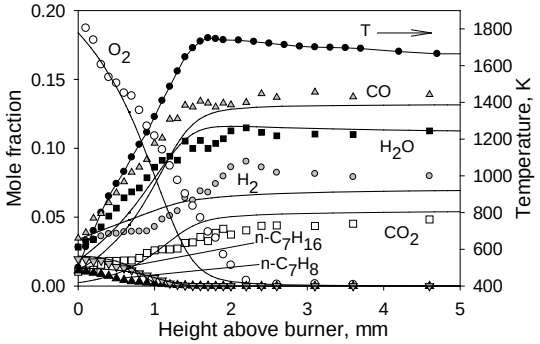

Fig. 4. Mole fraction profiles of reactants and major products in n-heptane/toluene/O_2/Ar flame. Symbols: experiment; curves: modeling.

Results and discussion

Simulated and experimental mole fraction variations vs. height above burner (HAB) for reactants and major products in the flame are given in Fig. 4. This figure also shows the measured temperature profile of the flame. As can be seen from the Fig. 4, the mechanism reproduces satisfactorily the concentration profiles of n-heptane, toluene, CO_2, CO, O_2, H_2O. Some discrepancies are observed between the measurements and the simulation results for

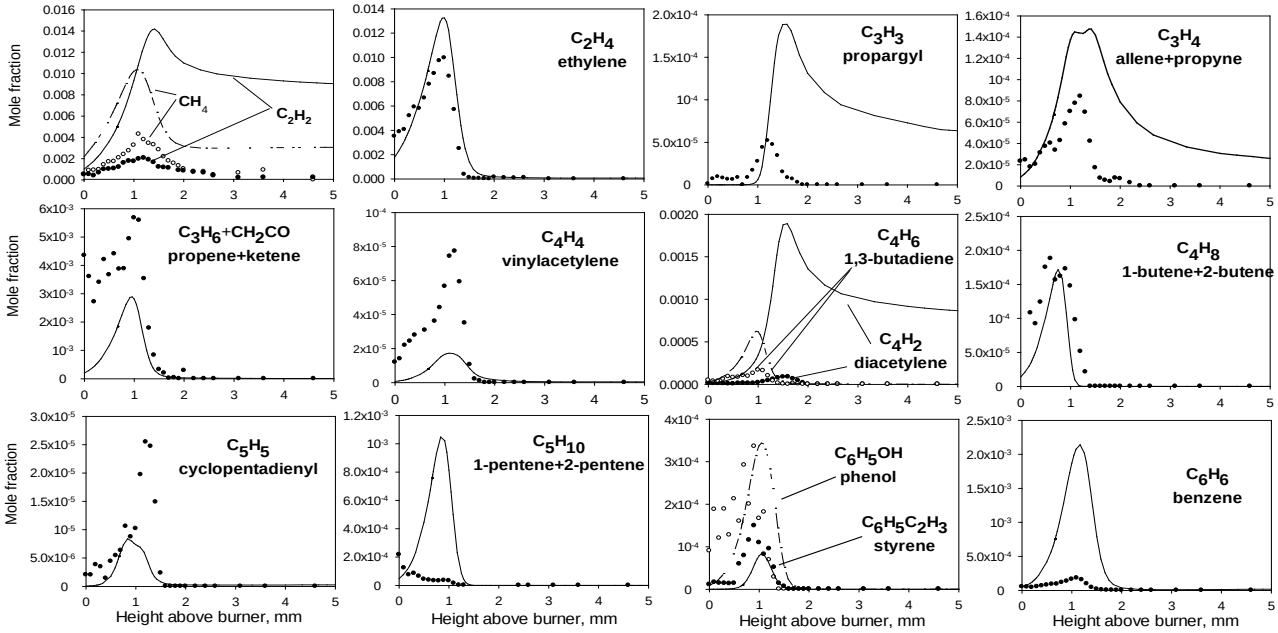

Figure 5. Mole fraction profiles of the main intermediates in premixed n-heptane/toluene/O_2/Ar flame. Symbols: experiment; curves: modeling.

H_2. This can be explained by high background signal at the mass peak m/z=2 due to the high diffusivity of hydrogen and, therefore, insufficient rate of H_2 evacuation from the vacuum system.

Figure 5 shows comparisons of the experimentally detected and simulated profiles of the species mole factions for: methane CH_4, ethylene C_2H_4, acetylene C_2H_2, propargyl C_3H_3, diacetylene C_4H_2, vinylacetylene C_4H_4, 1,3-butadiene C_4H_6, cyclopentadienyl C_5H_5, benzene C_6H_6, phenol C_6H_5OH, styrene $C_6H_5C_2H_3$. The species related to mass peaks 40 (allene+propyne), 42 (propene+ketene), 56 (1-butene+2-butene), and 70 (1-pentene+2-pentene) are not separated due to the very close difference between the ionization potentials of corresponding components. Measured and predicted profiles of combined mole fraction of these species are also given in Fig. 5.

As can be seen from the figure, the mechanism used predicts well the mole fraction profiles for the following intermediates measured: ethylene, butene (combination of isomers), phenol, styrene. However, it should be noted that for a few species (acetylene, diacetylene, 1-pentene+2-pentene) the mechanism does not provide an even qualitative agreement with the experimental data. In particular, the measurements demonstrate that acetylene and diacetylene are consumed completely in the post flame zone, however the model predicts a relatively high level of their mole fraction in this zone. Moreover, the model significantly overpredicts the maximum mole fraction of these species. It overpredicts more than twice the peak mole fractions for methane, propargyl, 1,3-butadiene,

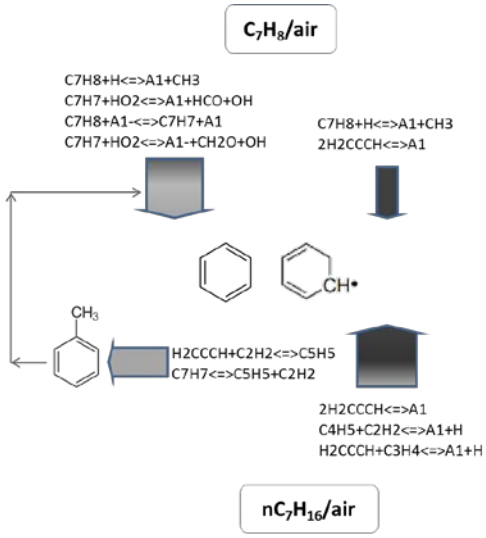

Fig.6. Schematic showing the reaction paths of formation of the first aromatic rings in toluene flame [10] versus n-heptane flame [9].

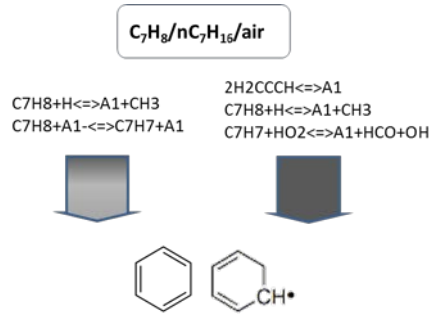

Fig.7. Main reaction paths of the first aromatic rings formation in the n-heptane/toluene flame studied in this work.

benzene; it underpredicts more than 2 times the peak mole fractions for propene+ketene, vinylacetylene, cyclopentadienyl.

To identify the reactions which have the most significant effects on the rate of benzene formation in the n-heptane/toluene flame studied in this work, a reaction path analysis is carried out. First, to better understand the origin of aromatic molecules formation, the pathways leading to benzene and phenyl formation in the n-heptane flame [9] (Fig.2) and in the toluene flame [10] (Fig.3) are analyzed (Fig.6) and then compared with those in the n-heptane/toluene flame studied (Fig.7). Three different flame zones (and flame temperatures) are examined: Preheat zone, main reaction zone, and post-flame zone. The thickness and color of pointers in Fig. 6 and 7 provide insights about the importance of the different reaction pathways and their relation to the flame zones. The darkest color corresponds to the post flame zone.

Fig. 6 illustrates that in the toluene flame the first aromatic ring formation in the preheat and main reaction zone occurs mostly through the reactions of H atom abstraction from toluene and reactions of benzyl radical with HO_2. In the post flame zone the reaction $C_7H_8+H<=>A1+CH_3$ dominates this process; propargyl radical recombination reaction becomes important as well. Unlike in the toluene flame, in the n-heptane flame, reactions of the small resonantly-stabilized radicals are the main routes to benzene (Fig. 6). The second non-negligible channel to the first aromatic ring formation is the benzyl production by recombination of cyclopentadienyl radicals with acetylene (Fig. 6). This route is most observable in the first flame zone.

As shown in Fig. 7 in the n-heptane/toluene flame the reaction paths to benzene are mostly similar to those plotted for the toluene flame in the Fig. 6. However in this case, in the post-flame zone, the reaction $2H_2CCCH<=>A1$ dominates and reaction $C_7H_7+HO_2<=>A1+HCO+OH$ becomes important as well. That can be explained with the high concentration of C_7H_7, which is produced in two parallel channels during the early stages of combustion: In the reactions of H abstraction from toluene and in the reaction $C_7H_7<=>C_5H_5+C_2H_2$, Fig.7. This means that the benzene formation pathways in the flame studied represent the combinations of routes observed in the individual flames, but dominated by the reaction paths typical for the pure toluene flame.

Acknowledgements

This work was partially supported by Russian Foundation of Basic Research under Grant No. 12-03-31246-a and EU Project FP7-265848-FIRST (Fuel Injector Research for Sustainable Transport).

References

1. N.A. Slavinskaya, U. Riedel, S.B. Dworkin, Q. Zhang, M.J. Thomson, Combust. Flame 159 (3) (2012) 979-995.
2. N.A. Slavinskaya, P. Frank, Combust. Flame 156 (9) (2009) 1705-1722.
3. N.A. Slavinskaya, B. Noll, Proceedings of GT2006ASME Turbo Expo 2006, GT2006-90958, Barcelona, Spain.
4. S. Heimel, R.C. Weast, Proc. Combust. Inst. 6 (1) (1956) 296-302.
5. S.G. Davis, C.K. Law, Proc. Combust. Inst. 27 (1) (1998) 521-527.
6. O.C. Kwon, M.I. Hassan, G.M. Faeth, J. Prop. Power 16 (3) (2000) 513-522.
7. Y. Huang, C.J. Sung, J.A. Eng, Combust. Flame, 139 (3) (2004) 239-251.
8. F. Inal, S.M. Senkan, Combust. Flame 131 (1-2) (2002) 16-28.
9. M. Tsurikov, K.P. Geigle, V. Krüger et al, Combust. Sci. and Tech. 177 (10) (2005) 1835-1862.
10. O.P. Korobeinichev, S.B. Ilyin, V.V. Mokrushin, A.G. Shmakov, Combust. Sci. Technol. 116-117 (1-6) (1996) 51-67.
11. I.E. Gerasimov, D.A. Knyazkov, S.A. Yakimov, et al., Combust. Flame 159 (5) (2012) 1840-1850.
12. T.A. Cool, K. Nakajima, K.A. Taatjes, et al., Proc. Combust. Inst. 30 (2005) 1681-1688
13. W.E. Kaskan, Proc. Combust. Inst., 6 (1957) 134-141.
14. C.R. Shaddix, Proc. of the 33rd National Heat Transfer Conference, HTD99-282, Albuquerque, New Mexico, 1999.
15. A.G. Shmakov, O.P. Korobeinichev, I.V. Rybitskaya, et al., Combust. Flame 157 (3) (2010) 556-565.
16. O.P. Korobeinichev, A.G. Tereshchenko, I.D. Emel'yanov, et al., Combust. Explo. Shock Waves 21 (5) (1985) 524-530.